RESOLVING THE ANGULAR PROFILE OF 60 GHZ WIRELESS CHANNELS BY DELAY-DOPPLER MEASUREMENTS

Erich Zöchmann, Sebastian Caban, Martin Lerch, and Markus Rupp

Christian Doppler Laboratory for Dependable Wireless Connectivity for the Society in Motion
Institute of Telecommunications, TU Wien, Austria
{ezoechma,scaban,mlerch,mrupp}@nt.tuwien.ac.at

ABSTRACT

Previous channel measurement campaigns in millimetre wave bands were mostly focussing on time invariant channels of static environments. Highly directive antennas were swept in azimuth and elevation angle to extract the angular profile of the double-directional radio channel. This angular profile is also visual in the Doppler domain. Therefore, contrary to common Doppler modelling, close scattering objects have to be taken into account. In this paper, a methodology for repeatable estimation of the angular profile through delay-Doppler measurements is proposed. Repeatable measurements of the static scenario allow for 1) optimization of the probing signals to reduce the geometrical effects and 2) disambiguation of the angular estimates through different measurement positions.

***Index Terms*—** Millimetre Wave, Doppler Effect, Angular Profile, Sparse Channel Modelling, Chirp

1. INTRODUCTION

The key assumption for millimetre wave (mmW) signal processing algorithms is a sparse multipath channel [1–4]. Previous works on millimeter wave channel sounding were mainly carried out indoors to exploit static environments [5–8]. Very few have also been carried out outdoors by equipping the transmitter and receiver with high gain horns and sweeping through azimuth as well as elevation to exhaustively search through all combinations [9]. Those measurements are naturally time consuming. They must rely on very long channel coherence times. Resolving the angular paths is also possible by the use of large arrays. To save hardware cost, most approaches use virtual arrays [10–12] and position a single receive antenna in order to emulate arrays. A different method, which has been given the least attention, takes advantage of the angular dependency of the Doppler effect. However, Doppler measurements suffer from angular ambiguities, hence multiple antennas [13] or multiple measurement positions must be used.

Delay-Doppler information is traditionally obtained from channel impulse response measurements [14–16]. From the time-variant impulse response $h(t,\tau)$, the Doppler-variant impulse response (delay-Doppler scattering function) $S(\nu,\tau)$ is calculated by Fourier transform. Through inspection of the spikes of the scattering function $S(\nu,\tau)$, the scattering objects can be resolved through different arrival times and different Doppler shifts [17]. The estimation of the scattering function is mostly performed by non-parametric periodogram based estimators, seldom by parametric ones [18]. Careful modelling of the Doppler effect uncovers a Doppler chirp due to close scattering clusters which are seen at changing angles during the observation time. Knowledge of this chirping suggests to treat the problem as chirp parameter estimation, see [19].

This work has been funded by A1 Telekom Austria AG and the Institute of Telecommunications, TU Wien. The financial support by the Austrian Federal Ministry of Science, Research and Economy and the National Foundation for Research, Technology and Development is gratefully acknowledged.

Our Contributions

In this contribution, we elaborate on estimating the Angle of Arrivals (AoAs) through Doppler measurements. Since scattering objects are in close proximity, we model the Doppler effect without the typical approximation that the angle between start and end of the observation interval is close to zero. Incorporating this angle reveals a Doppler chirp, which has to be dealt with. The probing signal is iteratively adapted to de-chirp the signal, thereby recovering the simple Doppler shift to AoA relation $\nu_D = \nu_{\max}\cos\alpha$.

In order to iteratively probe the wireless channel, we come up with a setup that allows for repeatable Doppler measurements. Furthermore, we propose to move the receiver in x and y direction. Through measurements on at least two different positions, the Doppler ambiguity can be resolved, which renders AoA estimation possible.

In Section 2, we propose a measurement methodology for controllable and repeatable measurements at relatively high speeds in static environments. We briefly introduce the frequently used (extended) Saleh-Valenzuela channel model and adapt it for our needs. We then focus on one propagation ray and study the effect of a moving receiver in Section 3. The occurring Doppler chirps hamper the detection of closely spaced scatterers. Clustering, as predicted by the channel model, might therefore not be verified by plain FFT based methods. Section 4 shows channel estimation techniques.

2. MEASUREMENT METHODOLOGY

The extended Saleh-Valenzuela model [20] is a popular choice for mmW signal processing algorithms [1, 21]. We adapt the original model to a time-variant directional SISO channel [15]

$$h(t,\tau,\alpha) = \sum_{l=1}^{L}\sum_{k=1}^{K} a_{l,k}\delta\big(\tau-\overline{\tau}_l-\tau_{l,k}\big)e^{j2\pi\nu_{\max}t\cos\left(\overline{\alpha}_l-\alpha_{l,k}\right)}\,, \tag{1}$$

where $\overline{\tau}_l, \overline{\alpha}_l$ is the mean delay and mean angle of arrival for the l^{th} scattering cluster and $\tau_{l,k}, \alpha_{l,k}$ is the delay and angle deviation of the k^{th} ray in the l^{th} cluster. The ray weights are denoted by $a_{l,k}$. The

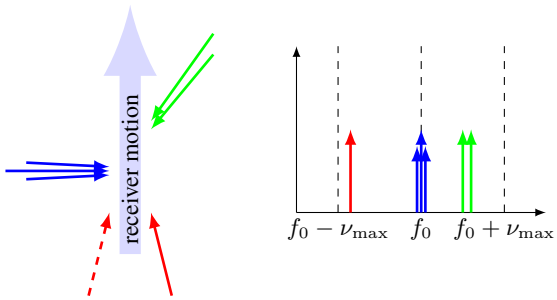

Fig. 1: Doppler spectrum of the extended Saleh-Valenzuela model.

Doppler spectrum associated to (1) is sketched in Figure 1; different cluster sizes are illustrated. The ray delays of one spatial cluster will not differ enough to distinguish them in the delay domain. Section 3 will model the observable Doppler spectrum (of on ray) to clarify whether rays are separable in the Doppler domain. The inherent left-right ambiguity is indicated with the dashed red arrow.

2.1. Calculation of Angle of Arrivals at Known Speeds

The relation between Doppler shift and AoA α is commonly described by $\nu_D = \frac{v}{c} f_c \cos\alpha = \nu_{\max} \cos\alpha$, hence

$$\pm\alpha = \arccos\left(\nu_D / \nu_{\max}\right) \ . \tag{2}$$

A second measurement at a shifted position is necessary to judge the sign in Equation (2). The accuracy of Equation (2) directly depends on the Doppler estimate. The receiver speed v offers a degree of freedom. Surprisingly, if we keep the length of the measurement segment l constant, the sampling rate Δf and the receiver speed v fall out of the equation. The number of sampling points is given by $n = \frac{l}{v}\Delta f$, thus the number of sampling points spent within $[-\nu_{\max}, \nu_{\max}]$ are

$$n_\nu = \frac{2\nu_{\max}}{\Delta f} n = 2\frac{v f_c}{c}\frac{1}{\Delta f}\frac{l}{v}\Delta f = 2\frac{f_c}{c} l \ . \tag{3}$$

As long the sampling theorem is obeyed, increasing the observation segment length l is the only way to improve Doppler resolution by FFT means. By increasing l, the underlying assumption of the common Doppler shift equation will be more and more violated.

2.2. Experimental Setup

Our experimental setup is based on [22] and the Vienna Wireless Testbed [23–25], which was used for evaluation of OFDM in [26–30]. The idea in a nutshell: "Linear translations are approximated by rotations to realize controllability and (fast) repeatability". The setup is based on a rotary arm, centred around a central pivot. The arm is moved with constant speed by an electric motor. Our setup is illustrated in Figure 2. For our mechanical dimensions, a measurement segment of $l = 0.5\,\text{m}$ approximates a linear translation with a height error of only 3.2 cm. We assume the electronics to withstand forces of 10g, which correlates to a circumferential speed of roughly 36 km/h. The whole rotatory unit is mounted on a sliding board which positions the device on an (x, y) grid.

To overcome high cable losses at 60 GHz, in a first step, the signal is down-converted to baseband. Therefore, an integrated circuit with a built-in antenna serves as RF frontend. The chipset is described in detail in [31]. The antenna is linearly polarized with 7.5 dBi gain and the antenna pattern is roughly $\cos^2(\theta)$ shaped (both azimuth and elevation) with a beamwidth of 120°. The in-phase and quadrature-phase baseband signals are transmitted over SMA cables and rotary joints to the baseband hardware.

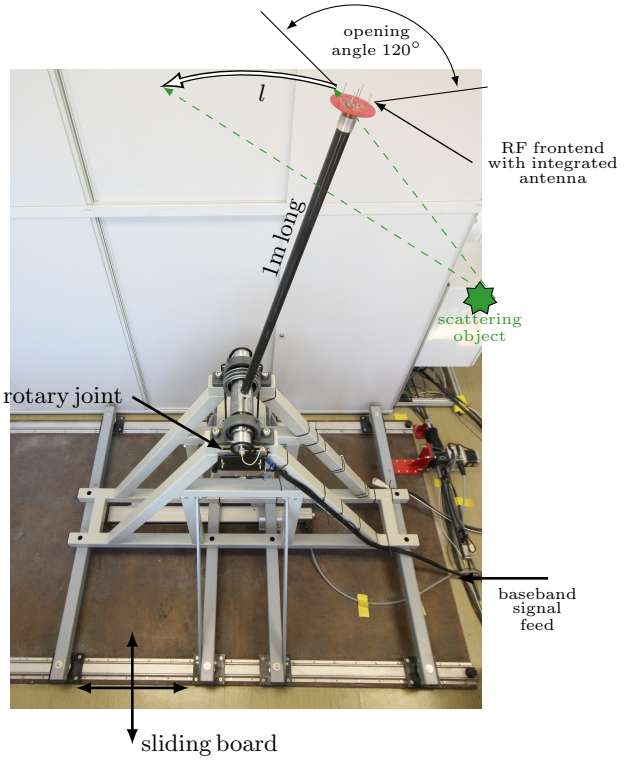

Fig. 2: Side view of the rotatory unit. A possible scattering object is indicated by the green star. Within the observation interval l/v, the scattering object is seen at a range of angles.

3. DOPPLER EFFECT MODELLING

A time-varying radial distance and therefore a time-varying delay $\Delta(t)$ between transmit and receive signal causes the Doppler effect. A single path received passband signal is modelled as [32]

$$y(t) = \text{Re}\left\{ A(\boldsymbol{r}(t))\, x\left(t - \Delta(t)\right) e^{j2\pi f_c (t - \Delta(t))} \right\} \ , \tag{4}$$

where A is the complex attenuation, $x\left(t - \Delta(t)\right)$ is the delayed transmit signal, and $e^{-j2\pi f_c \Delta(t)}$ is the Doppler shift, respectively.

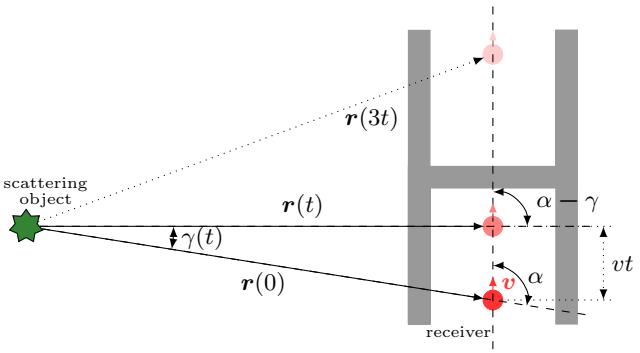

Fig. 3: Geometry for the 2D moving receiver Doppler effect calculation. Top view of the rotatory unit.

$$\tilde{y}(t) = Ax(t-\Delta(t)) \exp\left\{ -j\frac{2\pi f_c t}{c}\left(v\cos\alpha + \underbrace{\frac{2r(t)-r(0)}{2r(t)^2}}_{\approx \frac{1}{2r(t)}} v^2 t \sin^2\alpha + \frac{1}{2r(t)^2} v^3 t^2 \sin^2\alpha\cos\alpha \right)\right\} \tag{16}$$

Within this contribution, we assume that the complex attenuation does not change over small observation lengths, i.e. $A(\boldsymbol{r}(t)) = A,\ \forall\, t \in [0, T]$, so that the complex baseband signal reduces to

$$\tilde{y}(t) = Ax(t-\Delta(t))e^{-j2\pi f_c \Delta(t)}\,, \tag{5}$$

Without loss of generality we limit ourselves to a 2D geometry. The generalization to 3D scattering is straightforward by including an elevation angle. Figure 3 shows the geometry. The position of the receive antenna at time t can be calculated from its initial position $\boldsymbol{r}(0)$ and its velocity vector $\boldsymbol{v}$

$$\boldsymbol{r}(t) = \boldsymbol{r}(0) + t\boldsymbol{v}\,. \tag{6}$$

The radial projection onto the direction of the wavevector $\boldsymbol{e_k}$ is given as

$$\langle \boldsymbol{e_k}, \boldsymbol{r}(t)\rangle = r(0)\cos\gamma(t) + tv\cos\left(\alpha-\gamma(t)\right)\,. \tag{7}$$

Whenever vectors are written non-bold-faced, we implicitly take their lengths. Subtracting the initial delay $\tau_0 = \frac{r(0)}{c}$, one can calculate the time varying delay to

$$\Delta(t) = \frac{r(0)\cos\gamma(t) + tv\cos\left(\alpha-\gamma(t)\right)}{c} - \frac{r(0)}{c}\,, \tag{8}$$

and Equation (5) evaluates to

$$\tilde{y}(t) = Ae^{j\phi}x(t-\Delta(t))e^{-j\frac{2\pi f_c}{c}\left(r(0)\cos\gamma(t)+tv\cos(\alpha-\gamma(t))\right)}, \tag{9}$$

where $e^{j\phi} = e^{j\frac{2\pi f_c r(0)}{c}}$. Through Equation (6), the length of $\boldsymbol{r}(t)$ is given as

$$r(t)^2 = r(0)^2 + 2r(0)vt\cos\alpha + (vt)^2\,. \tag{10}$$

The law of cosines states

$$(vt)^2 = r(0)^2 + r(t)^2 - 2r(0)r(t)\cos\gamma(t), \tag{11}$$

which can be rearranged by (10) to[1]

$$\cos\gamma(t) = \sqrt{\frac{\left(r(0)+vt\cos\alpha\right)^2}{r(t)^2}} = \sqrt{1-\frac{(vt)^2\sin^2\alpha}{r(t)^2}} \tag{12}$$

$$\approx 1 - \frac{(vt)^2\sin^2\alpha}{2r(t)^2}\,. \tag{13}$$

The approximation (13) used the Taylor expansion of the square root around 1. Next $\cos\left(\alpha-\gamma(t)\right)$ is expanded to $\cos\left(\alpha-\gamma(t)\right) = \cos\alpha\cos\gamma(t) + \sin\alpha\sin\gamma(t)$ and the law of sines is evoked to find

$$\sin\gamma(t) = \frac{vt}{r(t)}\sin\alpha\,. \tag{14}$$

We finally arrive at

$$\cos\left(\alpha-\gamma(t)\right) \approx \cos\alpha - \frac{(vt)^2\sin^2\alpha}{2r(t)^2}\cos\alpha + \frac{vt}{r(t)}\sin^2\alpha. \tag{15}$$

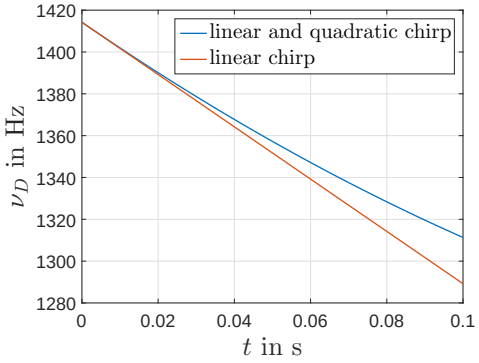

Fig. 4: Doppler chirp for $v = 10\,\frac{\mathrm{m}}{\mathrm{s}}$, $\overline{\alpha} = \frac{3\pi}{4}$ and $r(t) = 4\,\mathrm{m}$.

Using Eqs. (13) and (15), the received baseband signal (9) turns into (16). The time-depending Doppler shift thus becomes

$$\nu_D(t) = \frac{f_c}{c}v\cos\alpha \qquad (\nu_0)$$

$$+ \frac{f_c}{c}\frac{1}{2r(t)}v^2 t\sin^2\alpha \qquad (\nu_1 t)$$

$$+ \frac{f_c}{c}\frac{1}{2r(t)^2}v^3t^2\sin^2\alpha\cos\alpha\,, \qquad (\nu_2 t^2)$$

so that additionally to the angular dependent Doppler shift (ν_0), a linear ($\nu_1 t$) and a quadratic ($\nu_2 t^2$) Doppler chirp is visual. At medium speeds and short observation times, the linear chirp is dominating, cf., Fig. 4. The chirp terms also prohibit the use of a single Doppler shift value to calculate α. To determine the angle of arrival, one has to study the whole Doppler trajectory as in [33]. However, as the radial delay is bounded by $\Delta(t) \leq \frac{vt}{c}$, resolving the time-varying delay in the time domain needs scarcely reachable bandwidths.

4. CHANNEL ESTIMATION

The time-variant channel impulse response is implicitly given by (16). With the delay variable τ and initial delay τ_0 it can be expressed as

$$h(t,\tau) = A\delta(\tau-\tau_0-\Delta(t))e^{-j2\pi\left(\nu_0+\nu_1 t+\nu_2 t^2\right)t}. \tag{17}$$

For any practical system, the time dependent delay $\Delta(t)$ is in the order of tenths of nanoseconds and bandwidths of multiple GHz must be spent to observe it. We therefore approximate

$$h(t,\tau) \approx A\delta(\tau-\tau_0)e^{-j2\pi\left(\nu_0+\nu_1 t+\nu_2 t^2\right)t}. \tag{18}$$

If we further consider to drop ν_2, for a simplified discussion, we obtain

$$h(t,\tau) \approx A\delta(\tau-\tau_0)e^{-j2\pi\left(\nu_0+\nu_1 t\right)t}. \tag{19}$$

[1] At this point, one might be tempted to approximate $r(t) \approx r(0)$. Equation (11) can then be used to derive $\cos\gamma \approx 1 - \frac{(vt)^2}{2r(t)^2}$. This approximation is independent of the receive angle and is only close for $\alpha = 90°$.

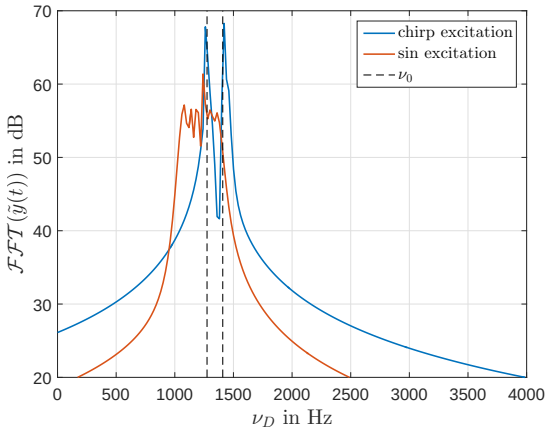

Fig. 5: Receive spectrum with sinusoidal and linear chirp excitation signal.

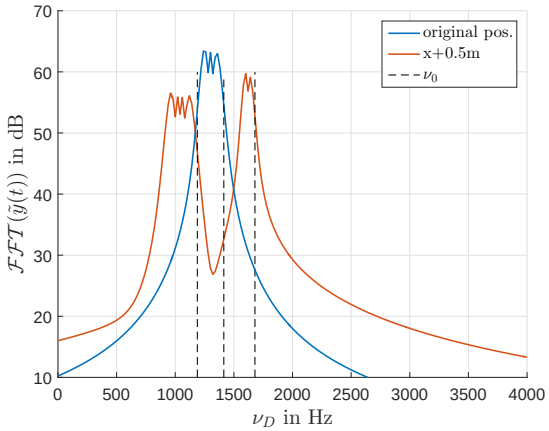

Fig. 6: Receive spectrum with two one-ray clusters at $\overline{\alpha_1} = 3\pi/4$, $\overline{\alpha_2} = -3\pi/4$, at ambiguous original position and at 0.5m shifted position.

Equation (19) describes now a linear chirp [34] with the Fourier transform [35]

$$S(\nu,\tau) = \int_{-T/2}^{T/2} h(t,\tau)e^{-j2\pi\nu t}\mathrm{d}t \tag{20}$$
$$= A\delta(\tau-\tau_0)\frac{1}{4}\sqrt{\frac{1}{\nu_1}}\exp\left[-j\frac{\pi}{2}\left(\frac{\nu-\nu_0}{\nu_1}\right)^2\right]\cdot F(T,\nu_0,\nu_1).$$

The Fresnel integrals $F(T,\nu_1,\nu_0)$ capture the time truncation T.

Generally, if the transmit signal $x(t)$ is designed such that it cancels the Doppler chirp, one would see a narrow spectrum, which allows resolving nearby rays. This principle is similar to linear frequency modulation matched filtering applied for RADARs [35, 36]. This can be seen by starting from Equation (19) and applying $x(t) = \exp(2\pi f_x t^2)$

$$\tilde{y}(t) = Ae^{j2\pi f_x(t-\tau_0)^2}e^{-j2\pi\left(\nu_0+\nu_1 t\right)t} \tag{21}$$
$$\approx Ae^{-j2\pi\left(\nu_0+(\nu_1-f_x)t\right)t} \overset{f_x=\nu_1}{=} Ae^{-j2\pi\nu_0 t} \tag{22}$$

In order to apply this ideal transmit chirp one has to know the impinging angles, which are subject of estimation. Assuming the ambience static within a couple of seconds, we can use the obtained knowledge from the first estimate to transmit a different probing signal, e.g., $t_{\mathrm{rep}} = \frac{2\pi}{v} = \frac{2\pi 1\,\mathrm{m}}{10\,\mathrm{m/s}} = 0.63\,\mathrm{s}$, later, relying on static channel conditions [37]. As the transmit signal is matched to the channel, we obtain the optimal SNR at the receiver.

An alternative to de-chirping would be to consider the problem as chirp signal estimation [19, 38, 39], or to take multiple snapshots, so that a sample covariance matrix can be used [40].

To demonstrate the Doppler chirping, we simulate a 2 ray cluster at $\overline{\alpha} = 3\pi/4$ with an angle deviation of 2.5° from the mean angle for each ray. The scattering cluster is at 4 m distance to the receiver. We measure on a segment of length $s = vt = 10\mathrm{m/s}\ 50\,\mathrm{ms} = 0.5\,\mathrm{m}$. The sample rate for resolving the Doppler spectrum can be chosen fairly low (if we ignore the delay resolution). Within these simulations, the sampling rate was set to 40 kHz. The Doppler spectrum of the sinusoidal excitation does not allow for judging the number of rays, see red solid line in Fig. 5. The probing signal (inverse-chirp) for the next iteration was designed using the already obtained spectrum matching the signal for one ray cluster[2]. Obviously, it is therefore neither perfectly matched to the first nor to the second ray. Although there is a small chirp remaining, both cluster rays are distinguishable now.

One weakness of Doppler based angular receive profile inference is the inherent ambiguity due to the symmetry of $\cos\alpha$ and $\sin^2\alpha$. In case the paths do not differ in their delays, there is no way to separate them later on. For sake of simplicity, the cluster consists now of just one ray. The measurement time and speed are chosen as before. The ambiguous estimation at the original position is shown in blue in Figure 6. Remember, our receiver is mounted on a slideable board. Therefore, a second measurement (shown in red) is obtained at a right-shifted position. The Doppler spectrum at the shifted position uncovers both clusters. The receiver was moved 0.5 m perpendicular to the rotating direction. Thus, the sign of the Doppler spectral shift verifies, that there has been a cluster in the left hemisphere (moved towards lower frequencies as the angle approaches 90°) and one in the right hemisphere (the angle moved towards 180°). Now, different chirp frequencies can be applied to improve the Doppler estimate of both clusters, as in the first example.

5. CONCLUSION

We have proposed a measurement methodology and hardware for estimating delay-Doppler scattering functions of mmW wireless channels. Precise modelling of the Doppler effect has shown that its estimation is not straight forward. Improvement through de-chirping has been confirmed. Even if more involved signal processing algorithms will be used, re-positioning is necessary to remove the inherent angular ambiguities.

6. REFERENCES

[1] O. El Ayach, S. Rajagopal, S. Abu-Surra, Z. Pi, and R. W. Heath, "Spatially sparse precoding in millimeter wave MIMO systems," *IEEE Transactions on Wireless Communications*, vol. 13, no. 3, pp. 1499–1513, 2014.

[2] R. Mendez-Rial, C. Rusu, N. Gonzalez-Prelcic, A. Alkhateeb, and R. Heath, "Hybrid MIMO architectures for millimeter wave communications: Phase shifters or switches?" *IEEE Access*, vol. PP, no. 99, pp. 1–1, 2016.

[2] We therefore need no prior knowledge on the cluster sizes.

[3] A. Alkhateeb, O. El Ayach, G. Leus, and R. W. Heath, "Channel estimation and hybrid precoding for millimeter wave cellular systems," *IEEE Journal of Selected Topics in Signal Processing*, vol. 8, no. 5, pp. 831–846, 2014.

[4] A. Sayeed and V. Raghavan, "Maximizing MIMO capacity in sparse multipath with reconfigurable antenna arrays," *IEEE J. Sel. Topics Signal Process.*, vol. 1, no. 1, pp. 156–166, June 2007.

[5] N. Moraitis and P. Constantinou, "Measurements and characterization of wideband indoor radio channel at 60 GHz," *IEEE Transactions on Wireless Communications*, vol. 5, no. 4, pp. 880–889, 2006.

[6] P. F. Smulders, "Statistical characterization of 60-GHz indoor radio channels," *IEEE Transactions on Antennas and Propagation*, vol. 57, no. 10, pp. 2820–2829, 2009.

[7] S. Geng, J. Kivinen, X. Zhao, and P. Vainikainen, "Millimeter-wave propagation channel characterization for short-range wireless communications," *IEEE Transactions on Vehicular Technology*, vol. 58, no. 1, pp. 3–13, 2009.

[8] E. Zöchmann, M. Lerch, S. Caban, R. Langwieser, C. F. Mecklenbräuker, and M. Rupp, "Directional evaluation of receive power, Rician K-factor and RMS delay spread obtained from power measurements of 60 GHz indoor channels," in *IEEE-APS Topical Conference on Antennas and Propagation in Wireless Communications (APWC 2016)*, Cairns, Australia, Sep. 2016.

[9] T. S. Rappaport, S. Sun, R. Mayzus, H. Zhao, Y. Azar, K. Wang, G. N. Wong, J. K. Schulz, M. Samimi, and F. Gutierrez, "Millimeter wave mobile communications for 5G cellular: It will work!" *IEEE Access*, vol. 1, pp. 335–349, 2013.

[10] M. Steinbauer, D. Hampicke, G. Sommerkorn, A. Schneider, A. F. Molisch, R. Thomä, and E. Bonek, "Array measurement of the double-directional mobile radio channel," in *Proceedings of Vehicular Technology Conferences*. IEEE, 2000.

[11] S. Ranvier, J. Kivinen, and P. Vainikainen, "Millimeter-wave MIMO radio channel sounder," *IEEE Transactions on Instrumentation and Measurement*, vol. 56, no. 3, pp. 1018–1024, 2007.

[12] J. Medbo, H. Asplund, and J.-E. Berg, "60 GHz channel directional characterization using extreme size virtual antenna array," in *26th Annual International Symposium on Personal, Indoor, and Mobile Radio Communications (PIMRC)*. IEEE, 2015.

[13] H. Thomas, T. Ohgane, and M. Mizuno, "A novel dual antenna measurement of the angular distribution of received waves in the mobile radio environment as a function of position and delay time," in *42nd Vehicular Technology Conference*. IEEE, 1992.

[14] G. Acosta, K. Tokuda, and M. A. Ingram, "Measured joint Doppler-delay power profiles for vehicle-to-vehicle communications at 2.4 GHz," in *Global Telecommunications Conference*. IEEE, 2004.

[15] R. S. Thomä, D. Hampicke, A. Richter, G. Sommerkorn, A. Schneider, U. Trautwein, and W. Wirnitzer, "Identification of time-variant directional mobile radio channels," *IEEE Transactions on Instrumentation and Measurement*, vol. 49, no. 2, pp. 357–364, 2000.

[16] A. Paier, J. Karedal, N. Czink, C. Dumard, T. Zemen, F. Tufvesson, A. F. Molisch, and C. F. Mecklenbräuker, "Characterization of vehicle-to-vehicle radio channels from measurements at 5.2 GHz," *Wireless personal communications*, vol. 50, no. 1, pp. 19–32, 2009.

[17] L. Bernadó, A. Roma, N. Czink, A. Paier, and T. Zemen, "Cluster-based scatterer identification and characterization in vehicular channels," in *11th European Wireless Conference*. VDE, 2011.

[18] S. M. Kay and S. B. Doyle, "Rapid estimation of the range-Doppler scattering function," *IEEE Transactions on Signal Processing*, vol. 51, no. 1, pp. 255–268, 2003.

[19] X.-G. Xia, "Discrete chirp-Fourier transform and its application to chirp rate estimation," *IEEE Transactions on Signal Processing*, vol. 48, no. 11, pp. 3122–3133, 2000.

[20] J. W. Wallace and M. A. Jensen, "Modeling the indoor MIMO wireless channel," *IEEE Transactions on Antennas and Propagation*, vol. 50, no. 5, pp. 591–599, 2002.

[21] E. Zöchmann, S. Schwarz, and M. Rupp, "Comparing antenna selection and hybrid precoding for millimeter wave wireless communications," in *IEEE 9th Sensor Array and Multichannel Signal Processing Workshop (SAM 2016)*, Rio de Janeiro, Brazil, Jul. 2016.

[22] S. Caban, J. Rodas, and J. A. García-Naya, "A methodology for repeatable, off-line, closed-loop wireless communication system measurements at very high velocities of up to 560 km/h," in *Instrumentation and Measurement Technology Conference*. IEEE, 2011.

[23] M. Lerch, S. Caban, M. Mayer, and M. Rupp, "The Vienna MIMO testbed: Evaluation of future mobile communication techniques," *Intel Technology Journal*, vol. 18, pp. 58–69, 2014.

[24] C. Mehlführer, S. Caban, and M. Rupp, "Cellular system physical layer throughput: How far off are we from the Shannon bound?" *IEEE Wireless Communications*, vol. 18, no. 6, pp. 54–63, December 2011.

[25] S. Caban, C. Mehlführer, G. Lechner, and M. Rupp, "Testbedding MIMO HSDPA and WiMAX," in *In Proc. of the 70th Vehicular Technology Conference Fall (VTC 2009-Fall)*, Sept 2009, pp. 1–5.

[26] M. Lerch, "Experimental comparison of fast-fading channel interpolation methods for the LTE uplink," in *Proc. of the 57th International Symposium ELMAR-2015*, Zadar, Croatia, Sep. 2015.

[27] R. Nissel, M. Lerch, and M. Rupp, "Experimental validation of the OFDM bit error probability for a moving receive antenna," in *IEEE Vehicular Technology Conference (VTC)*, Vancouver, Canada, Sept 2014.

[28] S. Caban, R. Nissel, M. Lerch, and M. Rupp, "Controlled OFDM measurements at extreme velocities," in *6th Extreme Conference on Communication and Computing*, Aug. 2014.

[29] R. Nissel and M. Rupp, "Doubly-selective MMSE channel estimation and ICI mitigation for OFDM systems," in *IEEE International Conference on Communications (ICC)*, London, UK, June 2015.

[30] J. Rodríguez-Piñeiro, M. Lerch, J. A. García-Naya, S. Caban, M. Rupp, and L. Castedo, "Emulating extreme velocities of mobile LTE receivers in the downlink," *special issue JWCN*, 2015.

[31] P. Zetterberg and R. Fardi, "Open source SDR frontend and measurements for 60-GHz wireless experimentation," *IEEE Access*, vol. 3, pp. 445–456, 2015.

[32] A. Napolitano, *Generalizations of cyclostationary signal processing: spectral analysis and applications*. John Wiley & Sons, 2012, vol. 95.

[33] R. J. Webster, "An exact trajectory solution from Doppler shift measurements," *IEEE Transactions on Aerospace Electronic Systems*, vol. 18, pp. 249–252, 1982.

[34] A. Springer, W. Gugler, M. Huemer, L. Reind, C. Ruppel, and R. Weigel, "Spread spectrum communications using chirp signals," in *EUROCOMM Information Systems for Enhanced Public Safety and Security*. IEEE, 2000.

[35] L. Varshney and D. Thomas, "Sidelobe reduction for matched filter range processing," in *Proceedings of the IEEE Radar Conference*, May 2003.

[36] C. Cook and M. Bernfeld, *Radar signals: An introduction to theory and application*. Artech House Publishers, 1993.

[37] M. Lerch, S. Caban, E. Zöchmann, and M. Rupp, "Quantifying the repeatability of wireless channels by quantized channel state information," in *IEEE 9th Sensor Array and Multichannel Signal Processing Workshop (SAM 2016)*, Rio de Janeiro, Brazil, Jul. 2016.

[38] D. S. Pham and A. M. Zoubir, "Analysis of multicomponent polynomial phase signals," *IEEE Transactions on Signal Processing*, vol. 55, no. 1, pp. 56–65, 2007.

[39] S. Barbarossa, "Analysis of multicomponent LFM signals by a combined Wigner-Hough transform," *IEEE Transactions on Signal Processing*, vol. 43, no. 6, pp. 1511–1515, 1995.

[40] B. Völcker and B. Ottersten, "Chirp parameter estimation from a sample covariance matrix," *IEEE Transactions on Signal Processing*, vol. 49, no. 3, pp. 603–612, 2001.